



## **CFD analysis of gas turbine combustor with vortex generator**

**Ulugbek Azimov, Saurabh Patil**

Mechanical and Construction Engineering Department, Northumbria University, Newcastle upon Tyne, NE1 8ST, United Kingdom.

Received 5 April 2017; Received in revised form 22 May 2017; Accepted 30 May 2017; Available online 1 Sep. 2017

### **Abstract**

Swirl flows have been used lately for the modern gas turbine combustion to enhance the mixing and flame stabilization. Instabilities that occur due to such flow are often termed as precessing vortex core (PVC). This precessing vortex core has a greater effect on the flow characteristics and heat release and its interaction with the flame is important. The numerical analysis using Reynolds-Averaged Navier-Stokes (RANS) and Large Eddy Simulation (LES) turbulence models were used to carry out simulations of gas turbine combustor to study the PVC and flame interaction in the flow fields. The boundary conditions were set as power output – 35 kW, Reynolds number - 52000 and the equivalence ratio - 0.65. The RANS results were more similar to the experimental one than the LES. The LES results were more useful in studying the PVC characteristics, PVC-flame interaction and instantaneous flow field. The RANS results were helpful in understanding the average flow fields. The grid requirement for both turbulence models and their importance was also studied.

**Copyright © 2017 International Energy and Environment Foundation - All rights reserved.**

**Keywords:** Gas turbine combustor; Vortex generator; CFD; LES; Precessing vortex core.

### **1. Introduction**

Swirl flame-stabilization technique is used for most of the gas turbine combustors nowadays. This technique has been evolved for the past decades to make the combustion more stable, clean and efficient. By the use of swirl flow in combustion, instabilities are developed in the fluid flow. These are hydrodynamic instabilities and are called precessing vortex core (PVC). This PVC phenomenon has been given much more attention in premixed combustion systems. PVC has a large effect on the flow field and to study its characteristics is very important. Not only the flow characteristics but also the flame interaction can be helpful to learn the overall combustion process and to improve the design of a combustor. The numerical approach for studying the combustion process is nowadays being extensively used in industries. The computational fluid dynamics (CFD) packages provide a wide range of turbulence models which can be used for flow simulation. The Reynolds-Averaged Navier-Stokes (RANS) turbulence models have a reasonable computational cost which makes them suitable to use.

The experimental set up of the gas turbine combustor equipped with different measuring techniques and instruments is mostly required to study the flow fields during the combustion. Such an experimental data suggests that, there are usually two types of flow patterns which can be observed during the combustion of a swirl burner. The first type is a large 3D instability which is time dependent called precessing vortex

core (PVC) and the second type is where this PVC amplitude is been damped by other with at least of 2 orders of magnitude. The occurrence of the first type of flow where the large PVC is present is at the non-reacting flow systems and where the mixture ratios are weak. The second type of flow pattern is seen where the turbulent diffusion flames are present [1].

In another experimental study, it says the PVC phenomena occur when the core of the vortex is displaced from the central axis of the symmetry, and a new centre of the vortex is formed. During the flow in the combustion chamber, a part of flow squeezes between outer wall of the burner and centre of the vortex. This affects the increase in tangential velocity. As a result, recirculation zones are formed around the centre of the vortex. The recirculation flow zones form a kidney shaped flow segment. During the combustion, the PVC also affects the temperature distribution. The results from the experiments suggest that the excitation of the PVC is under unusual condition i.e. in diffusion controlled condition [2]. The temperature fluctuation mainly occurs in the jet region of PVC. This is caused due to the turbulence and high shear which increases the mixing but does not allow the flame stabilization. The dynamics of the flow, like the PVC and the recirculation zones, enhances the flame stabilization.

Another experimental study performed using Laser Doppler Velocimetry (LDV) and Particle Image Velocimetry (PIV) at constant Reynolds number and the constant swirl parameter shows the trends of relevant variables which characterizes the flow field. In this experiment the analysis of velocity profiles, probability density function and power spectral density function were performed. From this study, it was gained that the turbulence intensity of small scale flow and the fluctuation which are periodic can be separated and are independent of  $G$ . The amplitude of the PVC is dependent on the Reynolds number and swirl parameter. The size of the precession region was not dependent on the Reynolds number [3].

In another study, high speed measurements of  $\text{OH}^*$  chemiluminescence and planar OH distribution were taken to describe heat release in combustion, flow field and flame-vortex interaction of a gas turbine combustor. In this combustor the flame was produced with the mixture of methane and air at an equivalence ratio of 0.75 producing a thermal power of 10kW. The thermo-acoustic frequency of the flow field was calculated to be 308 Hz. The PVC constrained the burner nozzle at a frequency of 515 Hz. At the thermo-acoustic frequency, the global heat release rate was seen fluctuated. The heat release centroid moved in the combustor at a frequency of 207 Hz. From this observation it was stated that the PVC and flame interaction has an effect on heat release. A double phase resolved statistics compilation was motivated to study the PVC-flame interaction. During this study, in the axial stretching of the PVC a contraction was observed at the minimum pressure and an extension at maximum pressure. The reaction zone stabilized where the incoming flow collided with the recirculation zone which is known as the stagnation line. The flow at other location showed deflection due to the presence of PVC. This deflection causes the fuel-jet having a better penetration in the direction of combustor walls [4].

The numerical simulation of gas turbine combustor was carried out by various researchers. The simulation efficiency and accuracy of results with the advanced simulation software makes it a reliable tool for an experimental study. In such an attempt, LES of the gas turbine combustor was performed. The results were then compared to the experiments. It was concluded that the flow field was more sensitive in the sub grid closure model. Vreman's model used in this simulation gave accurate results regarding inner and outer recirculation zones. The temperature profiles and mixture fraction shows the flame location and mixing [5].

In another simulation, based on Favre filtered conservation equation and for sub grid scale model, modified Smagorinsky model was used. The results provided by this turbulence model were in compliance with the measured and calculated velocity fields and turbulence properties. The PVC dominated the flow in this case. In the spiral vortex core the twist direction depended on the difference in the angular velocity beside the stagnation point. There were two swirlers, one co-rotating and another counter rotating. Both of them were examined to study the influence of swirler's direction. The counter rotating swirler was more effective in creating fuel-air mixture which led to efficient and a stable combustion. This was because of a shorter recirculation zone in the region of main atomization having stronger shear stress and the intensity of turbulence [6].

An assessment was done to unsteady RANS in the prediction of swirl flow instabilities. The swirl flow with swirl number 0.75 and Reynolds number which ranges from 10,000 to 42,000 were investigated both numerically and experimentally. From the results achieved it can be said that a full Reynolds stress model was able to make qualitative and quantitative predictions of PVC. In the U-RANS, the energy contained in the motion of PVC was expressively under predicted. When the computational cost was compared, 3D time dependent simulation was costly than the steady state RANS turbulence model [7].

Speziale [8] studied the numerical simulation of gas turbine combustor model using both U-RANS and LES turbulence model. From the results of this study it can be stated that the U-RANS method can be an effective alternative to LES. For LES a fine grid is required in all direction, and not only near the wall. A hybrid of LES-RANS was suggested where the RANS resolves a whole domain except a wall region which is resolved by LES. For predicting the combustion with LES the results can be improved by using advanced mixing models and chemistry models. The use of LES in the future will certainly increase and the URANS will be dominant in some of the specific industrial application.

## 2. Numerical configuration

### 2.1 Gas turbine combustor geometry of experimental setup

Figure 1 shows the schematics of gas turbine combustor that has been used as reference modeling and simulation. This gas turbine combustor was first investigated experimentally by [9]. The injector part of the combustor consists of a central nozzle, annular nozzle and the fuel nozzle. Through the central nozzle and the annular nozzle, the air flows into the combustor. For both the air nozzle, a swirling supply of air through the swirlers is done. The central air nozzle has a diameter of 15mm, annular air nozzle has an inner diameter of 17mm and outer diameter of 25mm. The fuel is supplied to the combustor through the fuel inlet. The fuel is of non-swirling nature. The fuel inlet is located between the central nozzle and the annular nozzle as seen in the Figure 1. The fuel nozzle is a ring of 0.5mm thick around the central nozzle. The exit plane of the annular nozzle and the central and fuel nozzle are 4.5mm apart. Due to this a partially premixed and lifted flame base is formed. The combustion chamber has square cross section of 85x85mm and a height of 110mm. The exhaust is tube of 40mm diameter and 50mm in height [10].

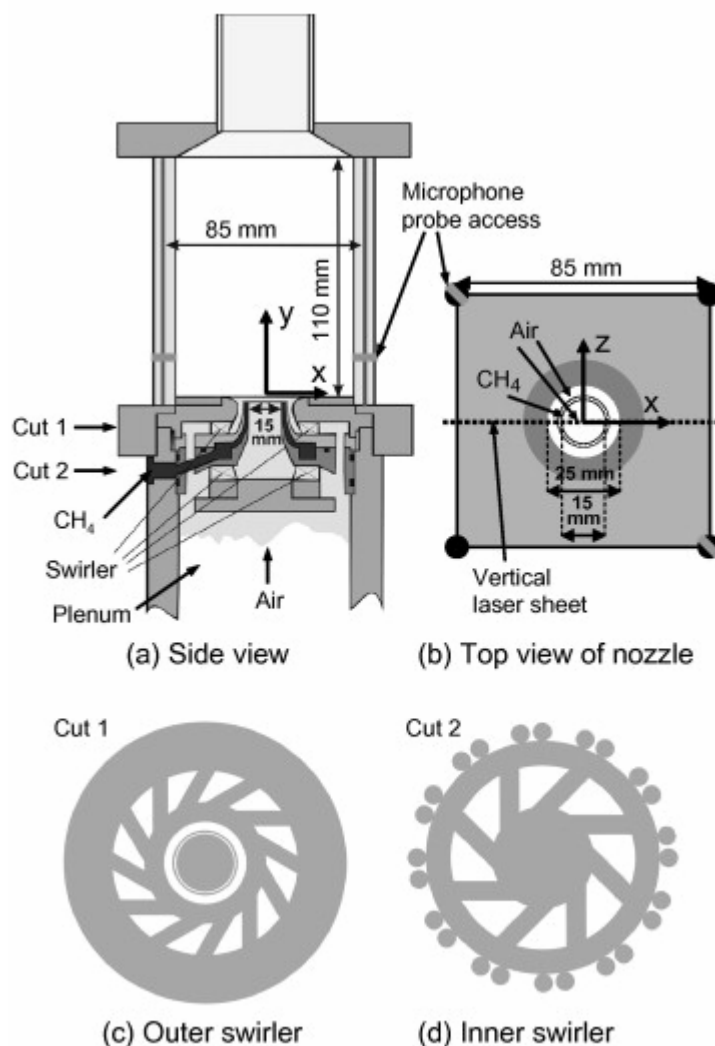


Figure 1. Experimental setup of gas turbine combustor [9].

The combustor model was discretized with tetrahedral unstructured mesh as shown in Figure 2. Total number of elements was approximately 3.1 million. Special care has been taken near wall as flow separation takes place in this part of the flow. The geometry was constructed as a single part instead of an assembly of various parts. The advantage of this was a continuous element structure which helps to avoid numerical instability. The overall size of the element was  $2e-03\text{mm}$ , which varies near the wall. Edge sizing was done where the flow from the swirlers enters the nozzle cross section. It can be seen in the figure where a dense mesh is present. This makes the mesh more refined and helps to obtain accurate results. The inflation option was applied to the swirler walls and the combustion chamber walls.

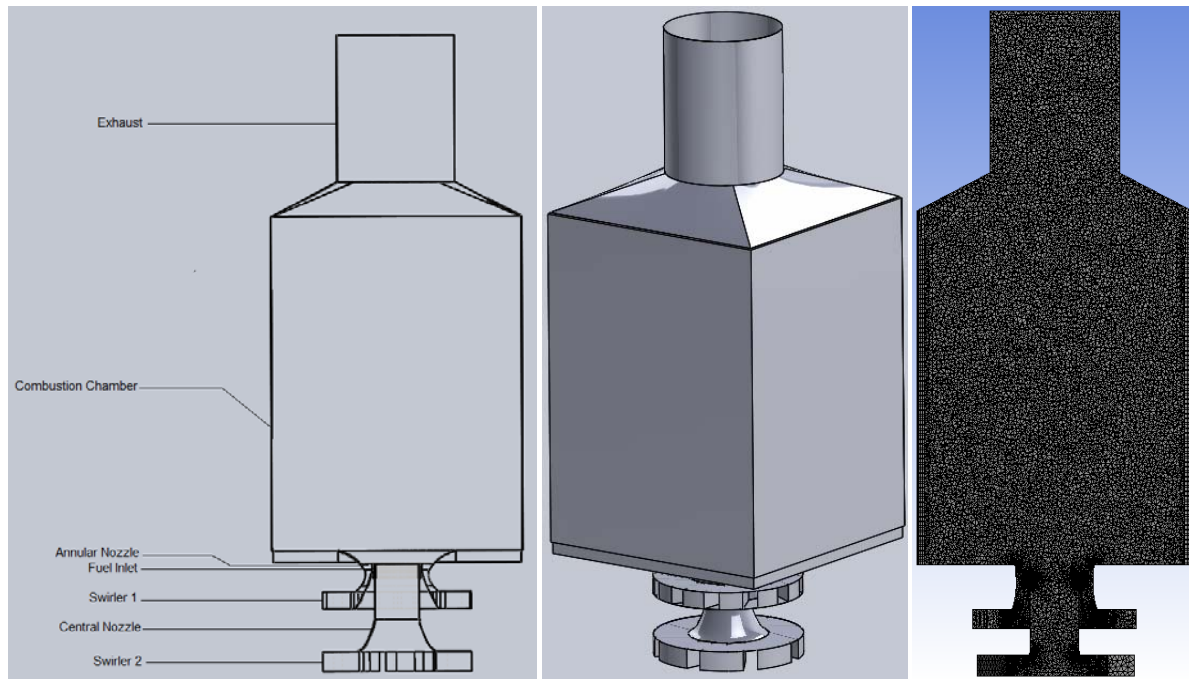


Figure 2. Schematics of gas turbine combustor model.

In the solution setup double precision option was used with 8-core processor. For carrying out the simulation, two turbulence models were used, namely  $k-\varepsilon$  and LES.  $k-\varepsilon$  model was used for finding the average velocity field non-reacting and reacting as well. The solver was set to pressure based type with absolute velocity formulation and transient time. The model was set to  $k-\varepsilon$  (standard) with a standard wall function. The constants were set to default. In species model, non-premixed combustion was set with adiabatic energy treatment. The energy equation was turned OFF and ON for non-reacting and reacting flows respectively. For the boundary conditions, there are two air-inlets and a fuel inlet. For the air-inlet 1 mass flow was  $0.01368\text{ kg/sec}$  with turbulent intensity set to 4.11%. For the air-inlet 2, mass flow was  $0.00456\text{ kg/sec}$  with the same turbulent intensity. For the fuel inlet, mass flow inlet was set to  $0.00069667\text{ kg/sec}$ . Annular to central nozzle air mass flow ratio was taken as 1.5 [9]. In solution initialization, a standard initialization was used and computed from fuel inlet. In the calculation settings, a time step was set to  $0.01\text{ s}$  with total 2500-time steps. Maximum number of iterations per time step was set to 10.

LES model was used for both reacting and non-reacting flow simulation. In case of non-reacting flow, the energy equation was turned off. The solver was pressure based with absolute velocity formulation and transient time. The model was set to LES with WMLES subgrid scale model for both non-reacting and reacting flows. For calculation settings, time step of  $0.002\text{ s}$  was taken and total 5000 time steps were set with maximum 10 iterations per time step. Same settings were used for reacting simulation, with the energy equation ON and total 10000 time steps were used.

The average velocity flow fields were well addressed from the results of selected turbulence models. The velocity components, like axial velocity, radial velocity and tangential velocity were compared with the experiments. The LES turbulence model with Algebraic Wall-Modeled LES Model (WMLES) subgrid-scale model was used. The instantaneous flow field and flame-PVC interaction were studied from the outcomes of this turbulence model. The geometry was discretized according to the need of solver and

turbulence model. The near wall boundary region was resolved well, as the LES turbulence model's requirement. The whole geometry was constructed as a single part rather than assembly. The boundary condition for both the turbulence model were same, that is equivalence ratio of 0.65, Reynolds number was set to 52,000 and the incoming mass flow rate of both air and fuel were taken from the experimental counterpart. There are 2 air nozzles, annular and central. The mass flow rate of the incoming air was divided in the ratio of 1.5 for annular to the central nozzle. The fuel inlet location was in between annular and central nozzle.

## 2.2 Numerical modeling

### 2.2.1 Reynolds-Averaged Navier Stokes (RANS)

The transport equation used in the ANSYS Fluent is as follows,

For  $k$ ,

$$\frac{\partial}{\partial t}(\rho k) + \frac{\partial}{\partial x_i}(\rho k u_i) = \frac{\partial}{\partial x_j} \left[ \left( \mu + \frac{\mu_t}{\sigma_k} \right) \frac{\partial k}{\partial x_i} \right] + G_k + G_b - \rho \epsilon - Y_M + S_k \quad (1)$$

For  $\epsilon$ ,

$$\frac{\partial}{\partial t}(\rho \epsilon) + \frac{\partial}{\partial x_i}(\rho \epsilon u_i) = \frac{\partial}{\partial x_j} \left[ \left( \mu + \frac{\mu_t}{\sigma_\epsilon} \right) \frac{\partial \epsilon}{\partial x_j} \right] + C_{1\epsilon} \frac{\epsilon}{k} (G_k + C_{3\epsilon} G_b) - C_{2\epsilon} \rho \frac{\epsilon^2}{k} + S_\epsilon \quad (2)$$

- $G_k$  represents turbulent kinetic energy generated due to the mean velocity gradients.
- $G_b$  represents turbulent kinetic energy generated due to buoyancy.
- $Y_M$  represents fluctuation dilation contribution in a compressible turbulence to overall dissipation rate.
- $C_{1\epsilon}$ ,  $C_{2\epsilon}$  and  $C_{3\epsilon}$  are constants.
- $\sigma_k$  and  $\sigma_\epsilon$  represent the turbulent Prandtl number for  $k$  and  $\epsilon$  respectively.
- $S_k$  and  $S_\epsilon$  are the source terms which are user defined.

The default values of the standard  $k$ - $\epsilon$  turbulent model constants are  $C_{1\epsilon}=1.44$ ,  $C_{2\epsilon}=1.92$ ,  $C_\mu=0.09$ ,  $\sigma_k=1.0$  and  $\sigma_\epsilon=1.3$

The  $k$ - $\epsilon$  standard model was used in this project to determine the average velocity field in the gas turbine combustor. The  $k$ - $\epsilon$  standard model performs well in determining various types of flows, but has some limits in its applicability. These limits arise due to the uncertainties in modelling of a turbulence production, turbulence transport and the assumption that are made in the modelling of dissipation rate equation. Some difficulties also arise while accounting for streamlines curvature, rotational strains and some other force effects.

### 2.2.2 Large Eddy Simulation (LES)

In LES, it is recognized that the large turbulence scales control heat/mass transfer, mixing etc., and the small turbulence scale are considered to understand their effect on the large scales. In LES, the governing equations are attained by filtering the Navier-Stokes equations which are time dependant. The Navier-Stokes equations are filtered in Fourier space i.e wave-number or configuration space. The filtered equations used in ANSYS Fluent in are given below,

$$\frac{\partial \rho}{\partial t} + \frac{\partial}{\partial x_i}(\rho \bar{u}_i) = 0 \quad (3)$$

and,

$$\frac{\partial}{\partial t}(\rho \bar{u}_i) + \frac{\partial}{\partial x_j}(\rho \bar{u}_i \bar{u}_j) = \frac{\partial}{\partial x_j} \left( \mu \frac{\partial \sigma_{ij}}{\partial x_j} \right) - \frac{\partial \bar{p}}{\partial x_i} - \frac{\partial T_{ij}}{\partial x_j} \quad (4)$$

In the above equations,  $\sigma_{ij}$  is stress tensor caused due to the molecular viscosity and  $\tau_{ij}$  is the sub grid scale stress. They both are defined as follows,

$$\sigma_{ij} \equiv \left[ \mu \left( \frac{\partial \bar{u}_i}{\partial x_j} + \frac{\partial \bar{u}_j}{\partial x_i} \right) \right] - \frac{2}{3} \mu \frac{\partial \bar{u}_l}{\partial x_l} S_{ij} \quad (5)$$

$$T_{ij} \equiv \overline{\rho u_i u_j} - \bar{\rho} \bar{u}_i \bar{u}_j \quad (6)$$

Subgrid-scale model: During the filtering operation in LES turbulence model, subgrid-scale stresses are formed and modelled. In ANSYS Fluent the subgrid-scale turbulence model employs the Boussinesq hypothesis. In case of the compressible flows, the density-weighted filtering operator is introduced. The subgrid scale stress from the above is split into the isotropic and deviatoric parts as,

$$\tau_{ij} = \underbrace{\tau_{ij} - \frac{1}{3} \tau_{kk} \delta_{ij}}_{\text{deviatoric}} + \underbrace{\frac{1}{3} \tau_{kk} \delta_{ij}}_{\text{isotropic}} \quad (7)$$

For the incompressible flows,  $\tau_{kk}$  term is either added to the filtered pressure or neglected. ANSYS Fluent offers 4 models for determining  $\mu_t$  as follows: 1) the dynamic Smagorinsky-Lilly model, 2) the Smagorinsky-Lilly model, 3) the WALE model, and 4) the dynamic kinetic energy subgrid-scale model. From above models, Algebraic Wall-Modelled LES Model (WMLES) was used. With WMLES the use of LES has a very less impact when industrial simulation is considered. The reason for this is very high resolution is required for wall boundary layer. This is why the LES is recommended for the flows where wall boundary layers are not so much important or where the boundary layers are laminar.

### 3. Results and discussion

#### 3.1 Average velocity field

Average velocity is shown in the Figure 3 for the vertical section. The mixture coming from the nozzle makes its way through the combustion chamber and due to its swirl nature forms an inner recirculation zone (IRZ) and an outer recirculation zone (ORZ). Due to the formation of IRZ and ORZ, a velocity gradient in the inner share layer between the inflow and IRZ is formed and also in the outer share layer between the inflow and ORZ.

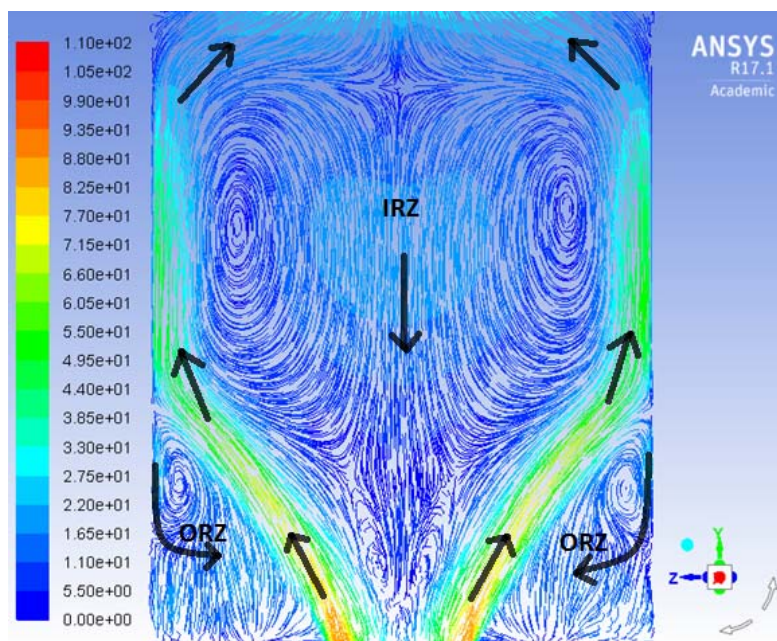


Figure 3. Average velocity field pathlines.

The formation of the recirculation zone is related to the flame stabilization. Due to formation of the recirculation zone, a low velocity region is created where the flame can be anchored. High level of velocity fluctuations can be seen in the areas of high velocity gradients in the inner shear layer (ISL) and outer shear layer (OSL). ISL is formed between the inflow and IRZ and the OSL is formed between the inflow and the ORZ. The strong velocity fluctuation can also be seen along the centre line in the upper part of the chamber. This velocity fluctuation is caused due to the vortex generated in the exhaust duct contraction.

In the average flow field shown in Figure 4, it is seen that the lower stagnation point (LSP) is located near the nozzle exit. This is important regarding to the precessing vortex core (PVC) and flame stabilization. At the LSP, the fresh gas coming from the nozzle collides with the burned gas from the IRZ. Thus the location of LSP is important as the reaction takes place and ignition is initiated. In LES flow fields the stagnation point location can be seen above the nozzle exit which will be discussed in further parts.

From the contour of the average velocity fields, the different vortices are seen which were not visible in Figure 3. Vortices present in the ISL have a specific effect on the flame front and its stabilization. Vortices are also seen in OSL but they have no effect on the flame. The vortices in the ISL are usually formed due to the PVC formation. Apart from the vortices in the ISL and OSL, they are also formed in exhaust of the combustion chamber. This is due to the contraction of exhaust path.

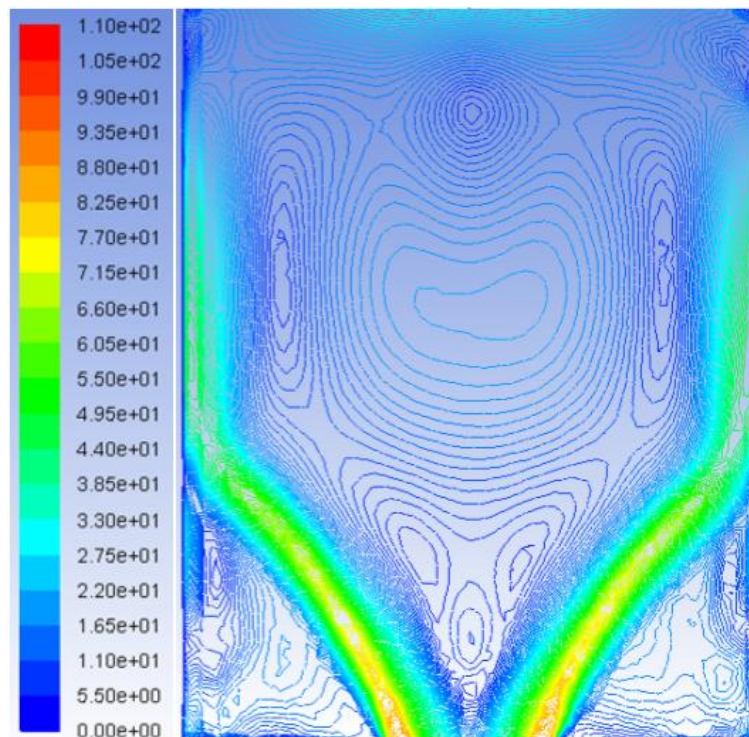


Figure 4. Average velocity field.

### 3.2 Instantaneous velocity field

Figure 5 shows the instantaneous velocity field. The small scale eddies, which were not visible in the averaged flow contour, can now be seen. The IRZ and ORZ are shown in the figure which can also be seen in average fields. Apart from them, the small eddies or vortices in ISL can be seen here. These vortices are of great importance in understanding the flame and vortex interaction. Also these vortices have an effect on the larger eddies as well. The vortices arrangement is in zig-zag manner and such arrangement of these vortices shows the presence of a helical vortex which is 3 dimensional. Such vortex is usually found in swirl flames and are known as precessing vortex core (PVC), which is going to be studied here [11].

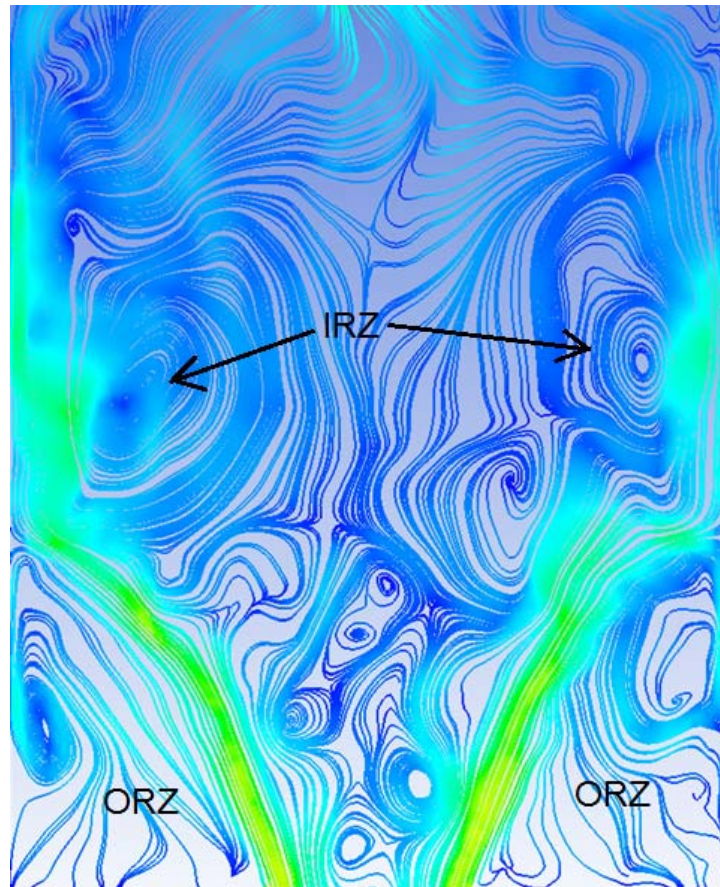


Figure 5. Instantaneous velocity field.

### 3.3 Representation of PVC

Figure 6 shows the PVC diameter at various levels in the combustion chamber. The streamlines of the velocity have been shown in the Y direction. Section (a) shows the changes with the position of its core on a plane located 2.5 mm from the bottom of the combustor. Small scale vortices can be seen around the incoming jet flow. The circle depicts the incoming flow from the air nozzles and the fuel nozzles. The circle can be seen enlarging as we go more further from the bottom. This is because the PVC in the middle pushes the coming flow in radial direction towards the wall. The PVC is the cause of the swirl flow and it is subject to the mixing of fuel-air and flame stabilization. Section (b) shows a plane located 5 mm from the bottom of the combustor in the same direction. The small vortices have been increased in their sizes and the incoming jet flow has moved towards the wall. The bigger circle suggests that the flow has moved forward. Where as for the PVC, the diameter is seen the same but the density of core has changed. In the experimental study, it has been stated that the diameter of the PVC has an influence of the heat release with dilatation [10].

In the plane located 20 mm from the bottom of the combustor, a large number of vortices can be seen. The diameter is increased in its size but the core density is being more dispersed. The PVC characteristics are being clear than before. The location of the PVC has been traced like small eddies seen in the transient flow field diagram, present in the inner shear layer showed a presence of instabilities in that part of the flow.

### 3.4 Temperature distribution

Figure 7 shows the superimposed images of temperature contour and the velocity vector. The colored part represents the temperature contour and the flame is located in the combustion chamber. From the figure it can be stated that the flame is stabilized in ISL, where PVC is located. Hence the PVC and flame interaction is strong because of their location. In the OSL, the vortex that is present here does not have much interaction with- and effect on flame. There are chances of some indirect effect on flame though. To study the characteristics of the flame, the different reaction zones have to be determined. The reaction zones are located at two regions: the first is at the stagnation point where the burned gas flow

from the IRZ collides with the fresh gas, and the second is near the vortices which causes the flames to roll up [10].

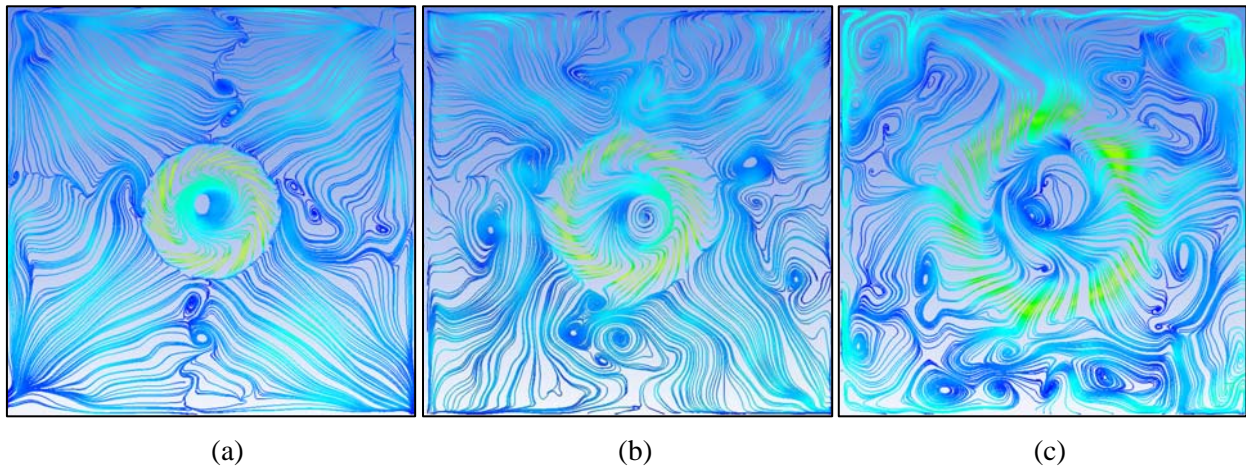


Figure 6. Precessing vortex core, (a) 2.5mm; (b) 5.0mm; (c) 20.00mm.

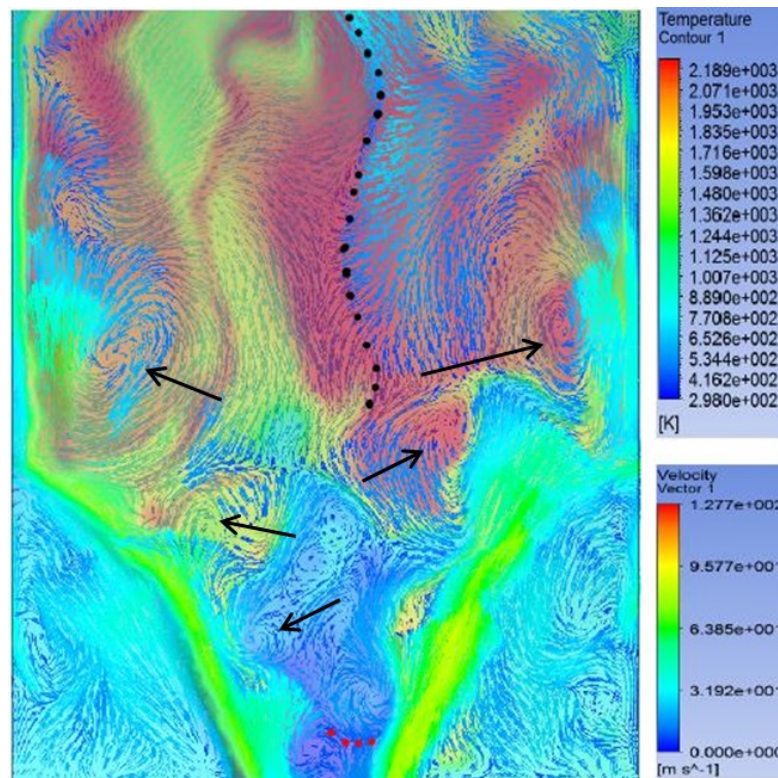


Figure 7. Temperature and velocity distribution and Vortices in Inner Shear Layer (ISL).

The red dots in the figure show where the stagnation takes place. It can be compared with the stagnation point located in the average velocity field, which was very near to the nozzle exit. The PVC has an impact on this stagnation line location and thus also affects the ignition. It causes high reaction rates near the stagnation points which supports in the proper burning of the coming fresh gas. Thus the opposed flow from the burned gases from the IRZ generates efficient supply of radicals and heat to newly coming unburned gas.

The figure shows the location of the vortices in the ISL. The vortices shown by the arrow has a significant effect on the flame. The vortices cause the flame to roll up and thus an enlarged flame surface can be seen. Due to the enlarged flame front more unburned gases come in contact with the flame and helps in burning and the reaction rate increases. The enlarged flame surface leads to the increase in the

mixing of the burned and unburned gases [12], thus enhances the ignition of unburned gases in ISL. After discussing both reaction zones, the ignition which takes place at the stagnation point serves as a source of ignition in the ISL reaction. The PVC induces both reactions and it can be noted that the PVC plays an important role in the combustion and flame stabilization.

### 3.5 Comparison with the experimental results

In this part, the velocity components namely axial velocity, radial velocity and the tangential velocity at different sections of the combustor have been calculated and compared with the experimental data. The comparison is done in the form of graphs, which clearly show the approximate resemblance in the results. But at some cases the deviation is seen and the reasons for this have been given below. Results shown here were taken from  $k-\varepsilon$  turbulence model. The LES graph comparison is shown in the appendix.

#### 3.5.1 Axial velocity

Figure 8 represents the axial velocity at 2.5 mm plane. The axial velocity is calculated by both the experiment and the numerical methods. The numerical graph trend is almost similar to that of experimental. The axial velocities are higher at 10mm from the centre. This is due to the incoming flow from the air nozzle located at this place. At most of the other places, it remains near 0m/s

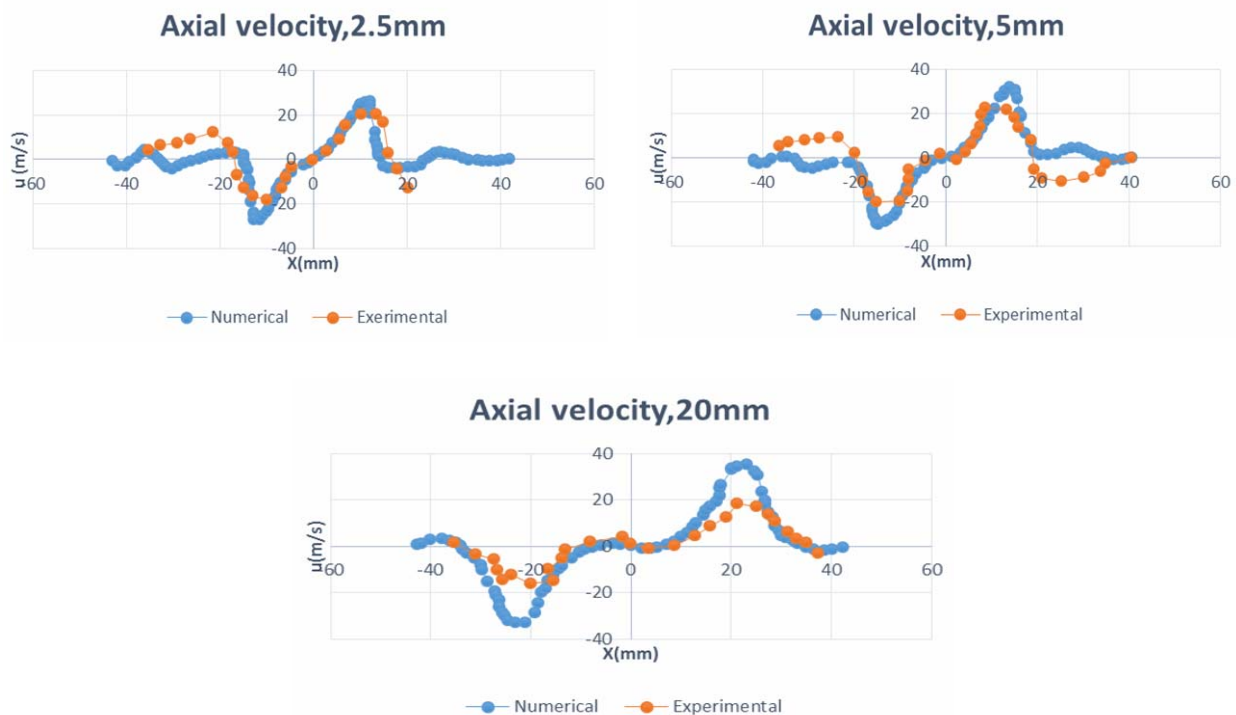


Figure 8. Axial velocity.

The axial velocity at 5 mm section also shows the same trend, which have high values around the 10mm from centre. Some deviations were seen at about 25-35 mm from the centre. Also the maximum value reached for the numerical calculation is higher than the experimental. At 20 mm, the axial velocity graph trend for the experimental results shows a decrease in the maximum value as the flows commences further into the combustor. But for the numerical results, this trend has not been followed. The values almost remain same for all the sections in numerical results. Another trend which can be seen is, shifting of the peak in the X direction. The peak values were observed at 10 mm X direction at 2.5 mm section, where as they got shifted to 20 mm X direction at 20mm section. This might be because of the incoming flow's direction towards the combustor walls.

#### 3.5.2 Radial velocity

Figure 9 shows the radial velocity at 2.5 mm section plane located from the bottom of the combustor. For both the experimental and numerical results the same trends were observed. The deviations were seen at

the peak velocities and the bottom end. The peak values were at approximately 10 mm from the centre. The deviation observed here were higher as compared to the axial velocity. The reason behind the peak values location is due to the collision of the incoming flow with the recirculation as well as the PVC causing them to move towards the wall.

The figure also shows the radial velocity at 5 mm section plane. The same trend is seemed to be followed in this case as well. But the deviation in this graph is greater as compared to the previous one. The deviation was not only seen at the peaks but also at the parts beyond 20 mm in X direction. The peak values are located at the same location. The graph at the 20mm section plane shows the same trend as for other two conditions. The peak values which were at 10 mm location in X direction were shifted to 20 mm in X direction. The peak value here shifted towards the wall is the same as with the axial velocity trend. The recirculation zone present in the central part causes the incoming flow to move towards the wall.

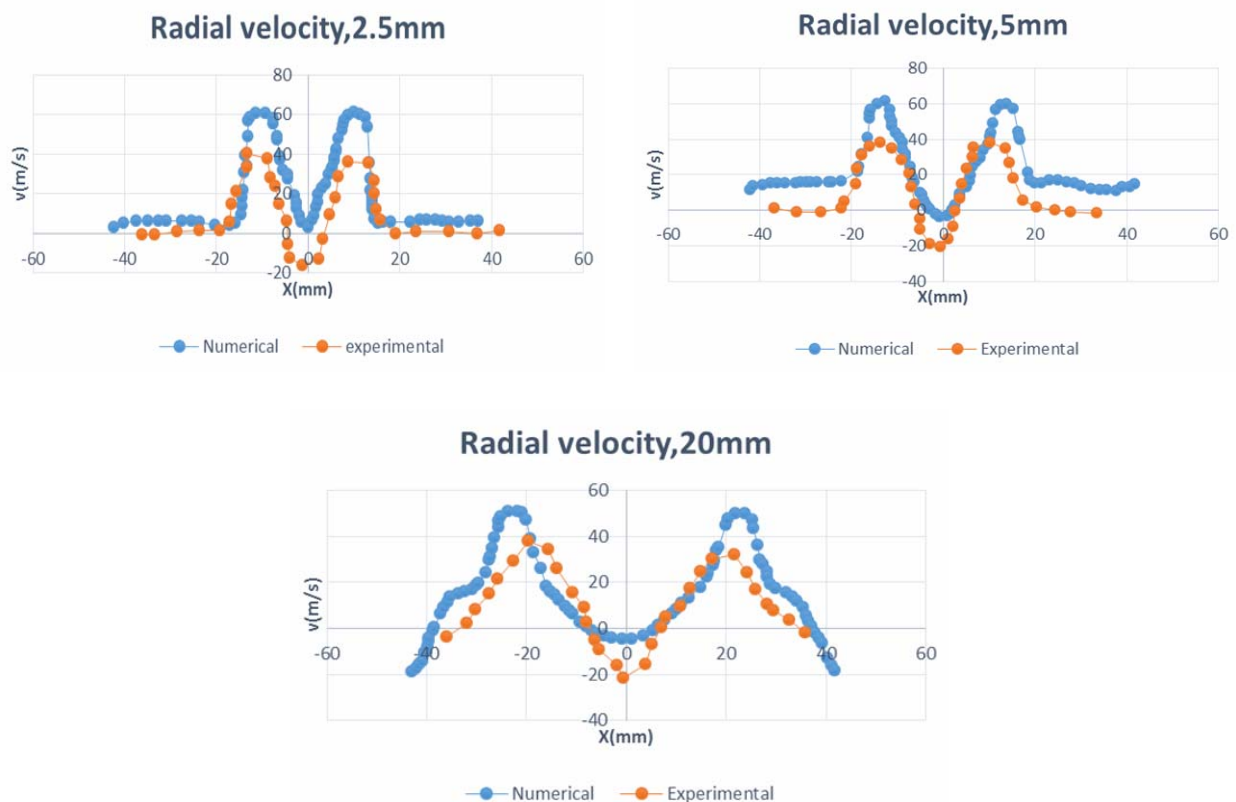


Figure 9. Radial velocity.

### 3.5.3 Tangential velocity

The tangential velocity is shown in Figure 10 at 2.5 mm section plane. The trend is somewhat similar to that of the axial velocity just in opposite way. The graph was not as smooth as in the other two cases.

At 5mm section plane the trend was changed and didn't resemble the former conditions. The deviation was seen at 20 mm X direction in the left hand side of the combustor. The graph shows the tangential velocity at 20 mm section plane with noticeable difference between experiment and simulation. The tangential velocity values are not as high as the axial and radial ones.

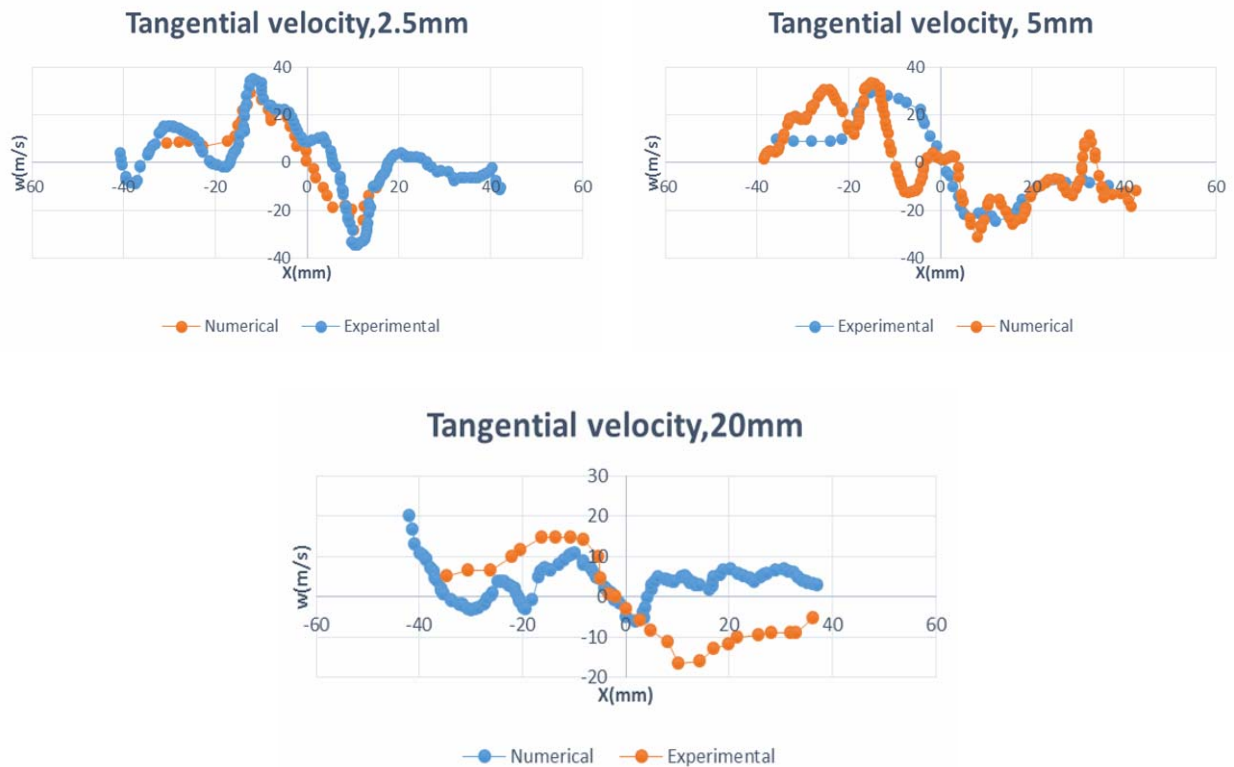


Figure 10. Tangential velocity.

#### 4. Conclusion

The numerical analysis of the gas turbine combustor was carried out using both the  $k-\epsilon$  (standard) and LES (WMLES) turbulence models. The same geometry and boundary conditions have been applied as in experimental work performed by Stohr et al [10]. The gas turbine combustor had a power output of 35 kW. The results from both models were used to show the characteristics of the PVC, flame-PVC interaction and the velocity component.

Due to a swirl flow a recirculation zones were created namely inner recirculation zone (IRZ) and outer recirculation zone (ORZ). This recirculation caused a region of low velocity where the flame was stabilized. The stabilization line was observed at the place where the incoming flow collided with the lower end of the inner recirculation zone. The velocity gradient generated shear layers. Inner shear layer was generated between the incoming flow and the IRZ and the outer shear layer was generated between the incoming flow and ORZ.

The vortices present in the inner shear layer shown in the instantaneous flow field suggest that there is presence of PVC in that region. Also the location of PVC shows that there is an interaction between the flame and PVC, because the flame is usually anchored near the inner shear layer. Vortex is also generated due to the contraction at the exhaust.

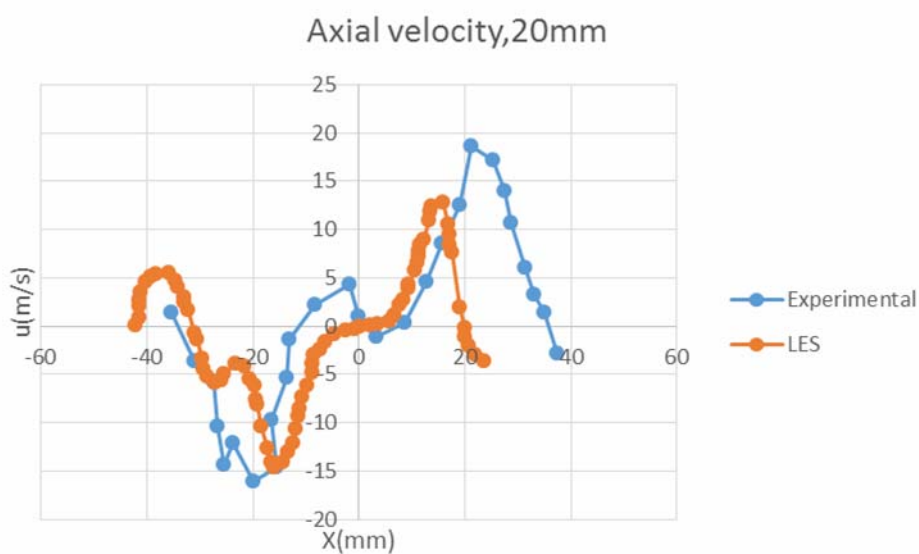
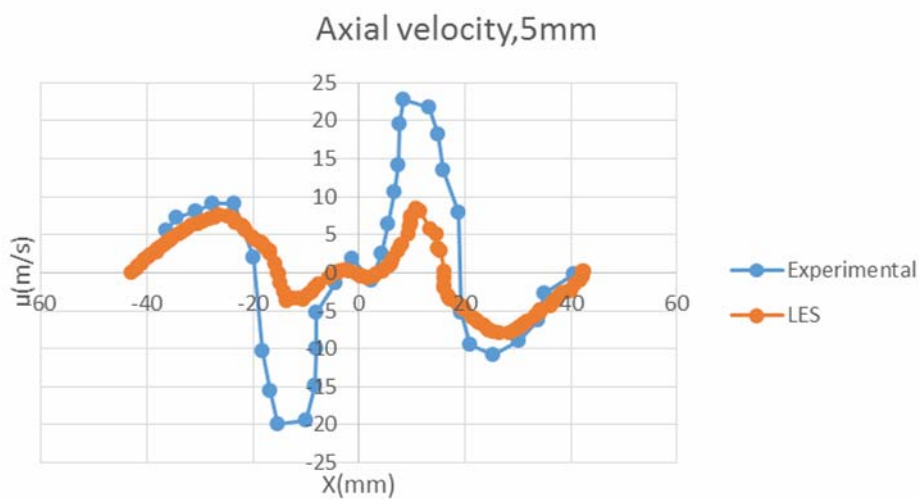
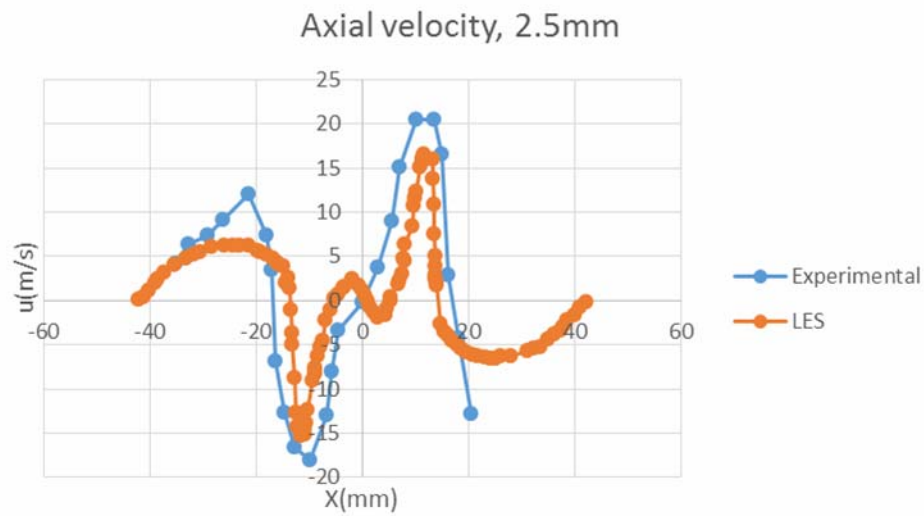
The exact location of the PVC is shown in the Y direction at various sections of the combustion chamber. The size of the PVC shows a slight increase. The PVC location keeps on changing in the vicinity. The flame-PVC interaction is strong in the IRZ.

The flame-PVC interaction was studied by determining the reaction zones in the combustion chamber. There are two reaction zones, one is at the stagnation point and another is at the vortices which causes the flame roll up. Due to the enlarged flame, the reaction rate is increased.

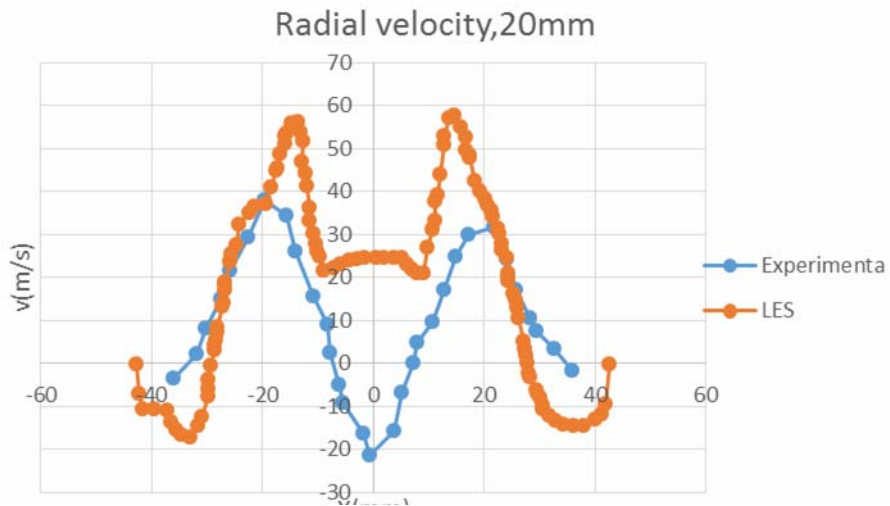
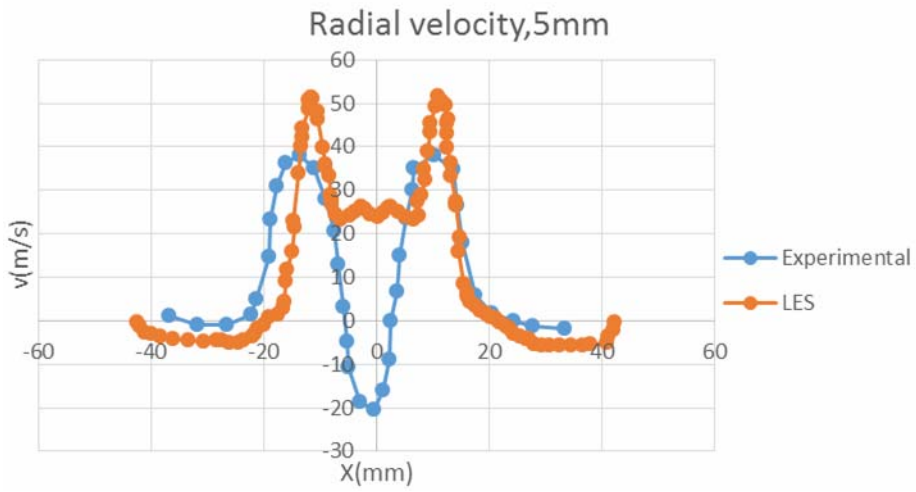
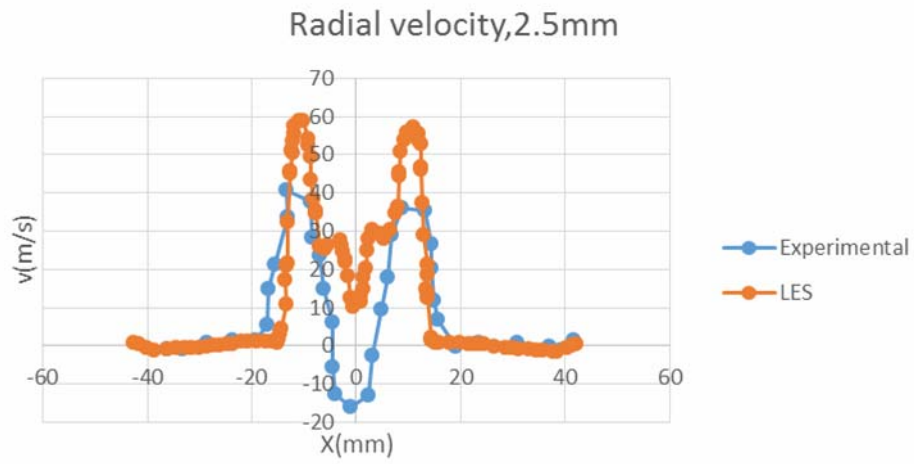
While comparing the velocity components, axial velocity, radial velocity and tangential velocity, the results showed the same trends with deviation at some places.

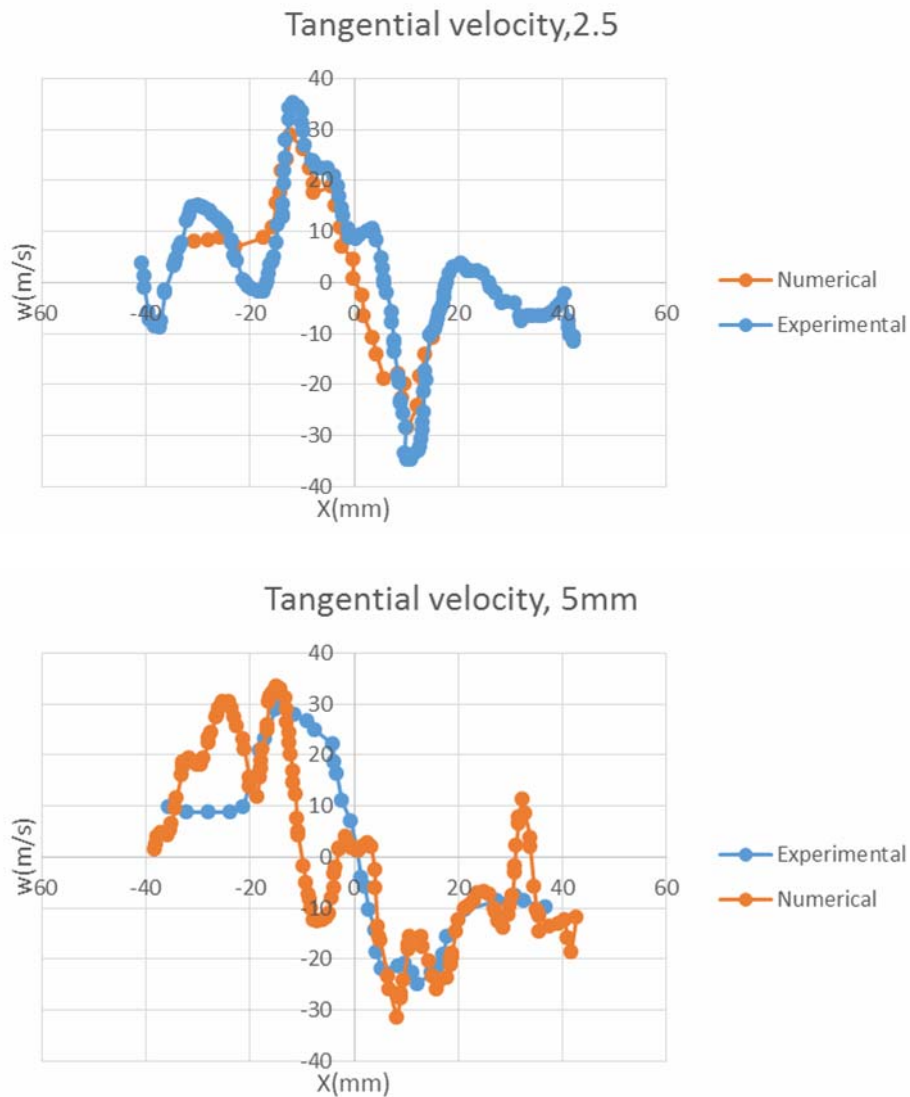
**Appendix**

## Large Eddy Simulation (LES) results

Axial velocity

Radial velocity



Tangential velocity**References**

- [1] Syred N., Gupta A.K., Beer J.M. Temperature and density gradient changes arising with the precessing vortex core and vortex breakdown in swirl burners. Symposium (international) on combustion, 1975, 15, 587-597.
- [2] Syred N., Fick W., O'doherty, T., Griffiths A.J. The effect of the precessing vortex core on combustion in a swirl burner. Combust. Sci. Technol., 1997, 125, 139-157.
- [3] Martinelli F., Olivani A., Coghe A. Experimental analysis of the precessing vortex core in a free swirling jet. Experiments in Fluids, 2007, 42, 827-839.
- [4] Steinberg A.M., Boxx I., Stöhr M., Carter C.D., Meier W. Flow-flame interactions causing acoustically coupled heat release fluctuations in a thermo-acoustically unstable gas turbine model combustor. Combust. Flame, 2010, 157, 2250-2266.
- [5] See Y.C., Ihme M. Large eddy simulation of partially-premixed gas turbine model combustor. Combust. Flame, 2015, 35, 1225-1234.
- [6] Wang S., Yang V., Hsiao G., Hsieh S.Y., Mongia H.C. Large-eddy simulations of gas-turbine swirl injector flow dynamics. J. Fluid Mechanics, 2007, 583, 99-122.
- [7] Wegner B., Maltsev A., Schneider C., Sadiki A., Dreizler A., Janicka J. Assessment of unsteady RANS in predicting swirl flow instability based on LES and experiments. Int. J. Heat and Fluid Flow, 2004, 25, 528-536.

- [8] Speziale C. Turbulence modeling for time-dependent rans and vles: a review. AIAA journal, 1998, 36, 173-184.
- [9] Weigand P., Meier W., Duan X., Stricker W., Aigner M. Investigations of swirl flames in a gas turbine model combustor: i. Flow field, structures, temperature, and species distributions. Combust. Flame, 2006, 144, 205-224.
- [10] Stöhr M., Boxx I., Carter C.D., Meier W. Experimental study of vortex-flame interaction in a gas turbine model combustor. Combust. Flame, 2012, 159, 2636-2649.
- [11] Syred N. A review of oscillation mechanisms and the role of the precessing vortex core (PVC) in swirl combustion systems. Prog. Energy Combust. Sci., 2006, 32, 93-161.
- [12] Cetegen B. Scalar mixing in the field of a gaseous laminar line vortex. Experiments in Fluids, 2006, 40, 967-976.



**Ulugbek Azimov** is a Senior Lecturer in Mechanical Engineering at the University of Northumbria, UK. He received his MSc degree in Mechanical Engineering from Texas A&M University, USA and PhD in Mechanical Engineering from Chonnam National University, South Korea. His research area includes combustion, alternative fuels, clean renewable energy systems and energy conversion and conservation. He is a fellow of Higher Education Academy UK.  
E-mail address: [ulugbek.azimov@northumbria.ac.uk](mailto:ulugbek.azimov@northumbria.ac.uk)



**Saurabh Patil** received MSc degree in Mechanical Engineering with distinction from Northumbria University, UK in 2017. He also received BEng degree from Shivaji University in Kolhapur India in 2015 and diploma in Automotive Engineering from New Polytechnic College in Kolhapur in 2012 both with distinction. Saurabh worked in various mechanical engineering design related projects. His main working field is CFD. Apart from CFD he has knowledge and expertise in mechanical stress analysis, vibration and product design and development.  
E-mail address: [saurabhpatil66@gmail.com](mailto:saurabhpatil66@gmail.com)